Military Technical College
Kobry El-Kobbah,
Cairo, Egypt.

16th International Conference on Applied Mechanics and Mechanical Engineering.

A NEW CONCEPT FOR THE LINE OF SIGHT STABILIZATION "BALL STABILIZATION"

H. F. Mokbel*, L. Q. Ying** and C. G. Hua***

ABSTRACT

For the purpose of directing the Line Of Sight (LOS) of Electro-Optical (EO) devices, two methods of Inertially Stabilized Platforms (ISP) are commonly used; the Mass Stabilization and the Mirror Stabilization. Whereas, in this research we present for the first time the new concept for the LOS stabilization, that we called "Ball Stabilization", which permits the angular rotations of the EO devices in the Azimuth and Elevation directions inside a spherical enclosure by using piezoelectric edge actuators and without the need of gimbals for each direction. The working principle, system analysis, conditions for optimal stabilization process, kinematics and dynamic modeling, and the experimental system are all discussed within this work. The elimination of gimbals has reduced the size and inertia forces of the system that facilitate the achievement of high resolution of $10^{-5º}$ within a compact size of 130 mm in diameter and a filed of view of ±30º in both directions, angular rates of $210^{º}$/s and angular acceleration of $24x10^{3º}$ /s^2.

KEY WORDS

Line Of Sight (LOS); Inertially Stabilized Platform (ISP); Piezoelectric Actuators;

* Egyptian Armed Forces. Email: hmokbel07@yahoo.com
** Assoc. professor, College of Mechanical and Electric Engineering, Changchun University of Science and Technology, China.
*** Professor, College of Mechanical and Electric Engineering, Changchun University of Science and Technology, China.

INTRODUCTION

The most specific definition for the Line Of Sight (LOS) between two objects is: "The vector between the sensor and a target" [1]. Whereas, in Electro-Optical (EO) Tracking, Ranging or Surveillance system, the Inertially Stabilized Platform (ISP) is used to isolate the LOS from carrier disturbance in order to guarantee accurate aiming and tracking for the target at the Inertial Space [2]. Two approaches are used to classify the LOS stabilization technologies; the 1st is according to the placement of the position and rate sensors, to Direct and Indirect Stabilization [3], and the 2nd is according to the moving parts, to Mass and Mirror Stabilization.

In the 1st approach; for the direct LOS stabilization, the position, rate and acceleration sensors are mounted directly on the LOS axis, i.e. on the laser beam lens or mirror. This configuration is mainly used in high precision applications [4-6], because it directly measures the disturbances about the axes of the LOS. In the indirect LOS stabilization configuration, the sensors are mounted on the gimbals base, which alleviates some complexity of the direct approach, but it is less efficient, since the disturbances are not measured in the LOS coordinate frame, which requires the transformation of these measures into equivalent disturbances about the LOS axis, also, several noise inputs are coupled to the platform disturbances.

While, in the 2nd approach; for mass stabilization, the massive EO devices perform the required rotations about one, two, or three axes through the same number of gimbals; of course increasing the number of gimbals will increase the volume and mass of the whole system [7-8]. This method can achieve wide range of rotations, but due to the massive structure and the consequently high inertia, the angular rates, accelerations, bandwidth, response, and settling time are usually limited to certain values [9]. In the mirror stabilization, the EO devices are connected to a fixed platform, while the optical beams falls on the reflecting surface of Fast Steering Mirror (FSM) with predetermined incident angle to reflect on this surface with the same incident angle to reach the target point. By changing the angular position of the FSM, the position of the optical beam will also change by twice the mechanical angle [10]. This method can achieve very high bandwidths due to the low inertia of the rotating masses, high accelerations and angular rate, higher precisions, fast response and settling times [11-12]. But, on the other hand they have limited angular rotations in the range of few mille radians, or in the best cases, few degrees on the expense of decreasing the bandwidth [13].

To take advantage of the strengths of each individual method, the regular decision is always using of both methods together, which is known as the augmented LOS stabilization. But, the increased size and complexity of the system are the main problems facing this trend. So, this research was directed to find out a new concept for the LOS stabilization that combines the advantages of both systems and avoids the weakness points. The new stabilization concept depends on the use of piezoelectric edge actuators to directly drive the payload. Piezoelectric actuators have the advantages of high power to size ratio, high holding force at zero power input, low inertia, fast start and stop, not affected by electromagnetic fields, non accompanying electromagnetic field, silent drive, Nano and sub Micrometer positioning.

WORKING PRINCIPLE

This new LOS stabilization concept depends on the rotation of the payload, that carrying the EO devices, inside a spherical enclosure. Where, the EO devices are assembled with the piezoelectric edge driving actuators and four sets of rolling rings in one compact and stiff structure that performs the rotation in the Azimuth and Elevation directions. Fig. 1 represents the two and three dimensional representations of this concept, where each pair of facing rollers contact the enclosure sphere in two points and are responsible for the rotation in one direction. This system simulates the human eye shape and rotation inside its cavity, where the tension of the muscles makes nearly pure rotation about the two axes orthogonal to the LOS's axis, with their origin fixed in the eye's center.

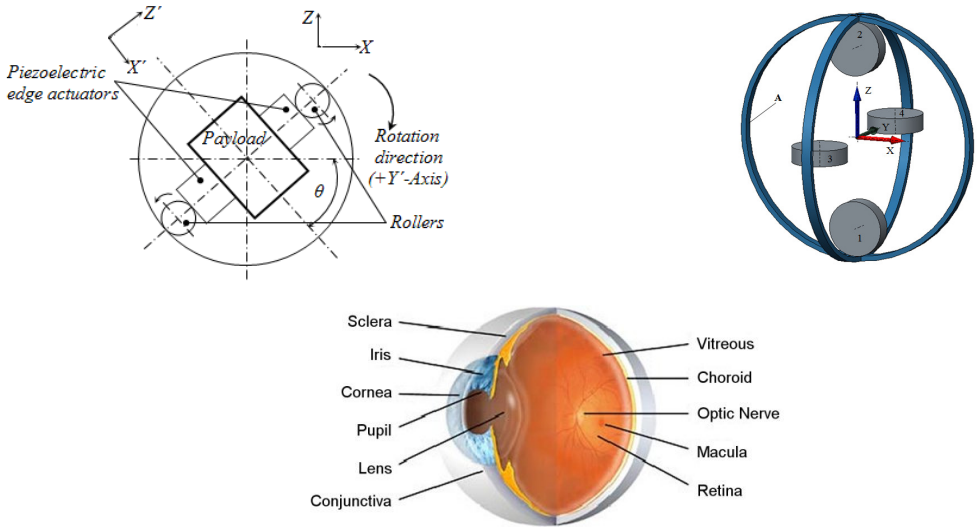

Fig.1. The Ball Stabilization Method working principle.

Each two sets of rolling rings have their rotation axis parallel to one axis of rotation of the whole system. The two-dimensional free body diagram shown in Fig.2 presents the enclosure sphere carrying the payload of weight W that acts at its Center of Rotation (CR), also the enclosure sphere is having an arbitrary elevation angle θ induced by the rotation of the carrier vehicle with an angular acceleration α_C , resulting in the new coordinate system of the sphere X□-Y□-Z□ and the applied moment $M=I_S\alpha_C$, (I_S is the mass moment of inertia of the rotating structure), that tends to rotate the structure relative to the sphere about the Y-axis of the sphere. Meanwhile, the braking forces B_1 and B_2 prevent the rollers to rotate about their center-axis and the frictional forces F_{f1} and F_{f2} prevent the inner structure from rotation relative to the enclosure sphere to keep the LOS of the EO devices fixed with the enclosure sphere during the driving actuators at rest and under the effect of outer torque disturbances from the carrier.

Moreover, the rotation of the rolling rings 1 and 2 by the rotating moment M_{r1} and M_{r2} produced by the linear forces T_1 and T_2 from the piezoelectric edge actuators, as shown in Fig.3.b, results in the rotation of the structure about its CR, that is coincide with its Center of Gravity (CG), which means the rotation about the Y-axis direction

that represents the Elevation direction. Consequently, the rotation of the rolling rings 3 and 4 will result in a similar rotation of the structure about its CR in the Z-axis direction which represents the Azimuth direction. In this case, the braking forces B_1 and B_2 are replaced by the driving forces T_1 and T_2, and the friction forces F_{f1} and F_{f2} work against the rotation motion of the rotating structure.

In all the above-mentioned discussion, the symmetry of the system plays an important role in simplifying the representation of the stabilization concept, where the CG of the rotating structure coincide with both the CR of the structure itself and the CG of the outer enclosure sphere.

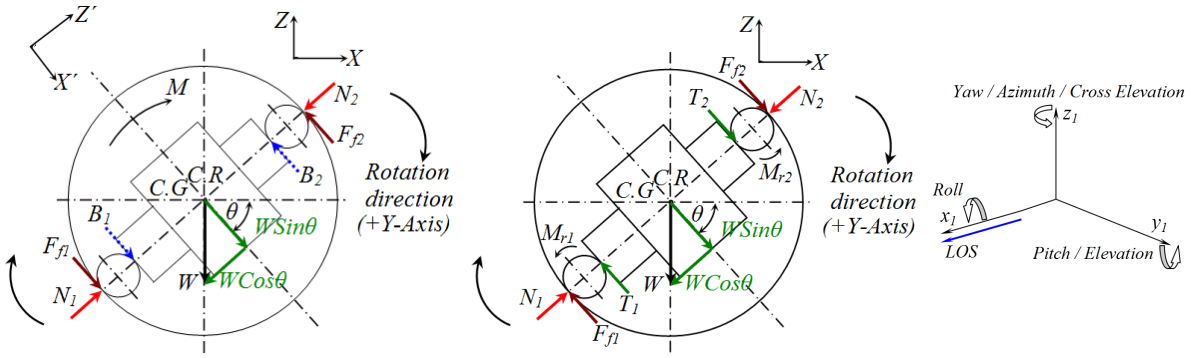

Fig.2. The two-dimensional free body diagram of the proposed system

SYSTEM ANALYSIS

The system analysis starts with determining the reactions from the inner ball surface onto the stabilization structure, then determining the applying forces and moments that works with and against the sliding and rotation motions for a certain rotation sequence. In all the following analysis, □, θ and ψ are the rotation angles about the X, Y and Z axes those represent the Roll, Elevation and Azimuth directions respectively.

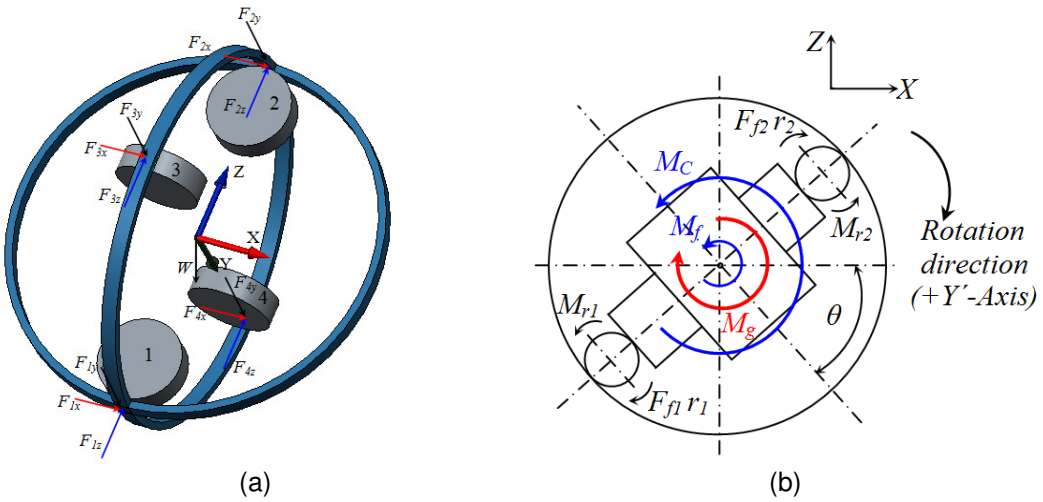

Fig.3. (a) Forces Acting on the Rollers during Rest, (b) Moments Acting on the Rotating Structure during Motion.

Forces Acting on the Rollers during Rest

The applied forces from the stabilization structure on the inner ball surface during rest are only the weigh *W* that has its direction fixed in the –Z-axis with respect to a fixed inertia reference frame. Whereas, the static holding force from the actuators on the four rollers that are denoted as the braking force (B_1, B_2, B_3 and B_4) are considered internal structural forces.

The rotating structure has four points of contact with the inner surface of the ball and the three dimensional reactions from the ball surface onto the contact points are F_{ix}, F_{iy} and F_{iz}, where *i=1:4* and stands for the number of the rolling ring.

$$F_{1x} = F_{2x} = F_{3x} = F_{4x} = W\,Cos\phi\,Sin\theta/4 \quad (1)$$

$$F_{1y} = F_{2y} = WSin\phi/4 \quad (2)$$

$$F_{3y} = (W\,Cos\phi\,Sin\theta + W\,Cos\phi\,Cos\theta + 2W\,Sin\phi)/4 \quad (3)$$

$$F_{4y} = (W\,Cos\phi\,Sin\theta + W\,Cos\phi\,Cos\theta)/4 \quad (4)$$

$$F_{1z} = (W\,Cos\phi\,Sin\theta + 2W\,Cos\phi\,Cos\theta)/4 \quad (5)$$

$$F_{2z} = W\,Cos\phi\,Sin\theta/4 \quad (6)$$

$$F_{3z} = F_{4z} = W\,Cos\phi\,Cos\theta/4 \quad (7)$$

The above equations are valid using the absolute values of θ and ϕ in the range of rotation from -90:0:90. While for the range of θ and ϕ from 90:±180:-90, besides using the absolute values, each $Cos\phi$ or $Cos\theta$ should have a negative sign. Also the reactions on each pair of rollers should be changed with each other. Also, the rotation around the Z-axis has no effect on the reactions since the weight force has always the –Z direction.

Moments Acting on the Rotating Structure during Motion

(1) Due to the incident rotation of the carrier vehicle with an angular acceleration α_C, with respect to the fixed inertia reference frame, the enclosure ball will have the same angular acceleration's value and direction, resulting in applying a moment M_C from the carrier onto the rotating structure.

$$M_C = I_S \alpha_C \quad (8)$$

(2) The applied forces from the actuators *T* result in driving moments from the actuators on the rollers M_r. The summation of those driving moments on the rollers results in a driving moment M_g from the actuators onto the rotating structure.

$$M_{(r1,r2,r3,r4)} = T_{(1,2,3,4)}\ r_{(r1,r2,r3,r4)} \quad (9)$$

$$M_{(g1,g2,g3,g4)} = M_{(r1,r2,r3,r4)}\ r/r_{(1,2,3,4)} \quad (10)$$

where,

r …….. Inner radius of the enclosure ball,

$r_{r1,r2,r3,r4}$ …Distance from the point of application of the actuator to the CR of the roller,

$r_{1,2,3,4}$……. Radii of the rollers

(3) Due to the rotation of the rollers on the inner surface of the surrounding ball, there appear frictional forces F_f between the rollers and the inner surface, resulting in friction moments M_f opposing the rotation of the rotating structure.

$$F_f = \mu\ N \tag{11}$$

$$M_{fx} = \mu\ r\ [F_{1z} + F_{2z} + F_{3y} + F_{4y}] = \mu\ r\ W\ [Cos\phi\ Sin\theta + Cos\phi\ Cos\theta + Sin\phi/2] \tag{12}$$

$$\begin{aligned} M_{fy} &= \mu\ r\ [F_{1z} + F_{2z}] + \mu\ r_o [F_{3y} + F_{4y}] \\ &= (\mu\ W/2)[r(Cos\phi\ Sin\theta + Cos\phi\ Cos\theta) + r_o(Cos\phi\ Sin\theta + Cos\phi\ Cos\theta + Sin\phi)] \end{aligned} \tag{13}$$

$$\begin{aligned} M_{fz} &= \mu\ r\ [F_{3y} + F_{4y}] + \mu\ r_o [F_{1z} + F_{2z}] \\ &= (\mu\ W/2)[r(Cos\phi\ Sin\theta + Cos\phi\ Cos\theta + Sin\phi) + r_o(Cos\phi\ Sin\theta + Cos\phi\ Cos\theta)] \end{aligned} \tag{14}$$

where,
μ ….. Coefficient of static or kinetic friction,
N …. Normal reaction force on the rigid surface,
r_o …. Pivoting radius of the rollers on the inner surface of the ball

Forces Participated in the System, but Having No or Minor Effects

There are some forces participated in the system's dynamics, but still having no or minor effects on the system and can be dropped off the analysis:

(1) The Rolling Resistance Force ($F_{rr} = C_{rr} N$) that results from the deformation of the rolling object or the rolling surface, and is very small compared to the friction forces, since the coefficient of rolling resistance $C_{rr} \approx 0.002$.

(2) Gravity torques (T_g) about each axis of the rotating structure, which has no effect since the axes of the CG of the body are aligned with the CR axes.

(3) Inner friction and cable restraint torques (T_f) which constructing the major part of the disturbances, and can be attenuated by the servo loop gain without the exact knowledge of viscous and cable restraints coefficients *(K_f and K_c)* if the rate loop bandwidth is such that [3]:

$$2\pi\ f_{ry} >> \left(K_f / I_y\right) \quad , \qquad (2\pi)^2 f_{ry} f_{ly} >> \left(K_c / I_y\right) \quad \text{And} \qquad f_r = \left(-1.196\zeta + 1.85\right) f_n$$

where
f_{ry} …… Elevation rate loop bandwidth.
f_{ly} …… Elevation rate loop lead frequency (≈ *1/3: 1/4 fry*)
f_n …… Natural frequency
ζ ……. Damping ratio (*0.3 ≤ ζ ≤ 0.8*)

$$T_f = k_f\ \dot{\theta} + T_{fn} + k_c \theta + T_{cn} \tag{15}$$

T_{fn}……..Nonlinear friction torques,
T_{cn}…….Nonlinear cable restraint torques.

CONDITIONS FOR OPTIMAL LOS STABILIZATION PROCESS

To guarantee the optimal working conditions for the Ball stabilization process and assure the absences of any undesirable motions, the system must satisfies the following conditions:

(1) ***When the actuators and carrier are at rest*****,** to prevent the undesirable relative slipping between the rollers and the inner surface of the ball, the applied moments on the rotating structure due to the reaction forces between the rotating structure and the enclosure sphere must be under equilibrium to maintain its position:

$$\sum M_x = F_{1y}r - F_{2y}r - F_{3z}r + F_{4z}r = 0 \quad (16)$$

$$\sum M_y = -F_{1x}r + F_{2x}r = 0 \quad (17)$$

$$\sum M_z = F_{3x}r - F_{4x}r = 0 \quad (18)$$

(2) ***During the actuators' rest, while the outer carrier is moving*****,** to prevent the undesirable relative slipping between the rollers and the actuators' braking forces, the moments applied on the rolling rings from the braking force must be higher than the moments applying on them due to the inertia forces caused by the rotation of the outer carrier:

$$(B_1 r_{r1} + B_2 r_{r2}) \succ M_{Cy} \quad , \quad M_{Cy} = I_{Sy}\alpha_{Cy} \quad (19)$$

$$(B_3 r_{r3} + B_4 r_{r4}) \succ M_{Cz} \quad , \quad M_{Cz} = I_{Sz}\alpha_{Cz} \quad (20)$$

(3) ***During the actuators' rest, while the outer carrier is moving*****,** to prevent the undesirable relative slipping between the fixed rollers of the rotating structure and the inner surface of the ball, the static friction moments resulting from the normal reactions forces between the rotating structure and the enclosure sphere must be higher than the moments applying on rotating structure due to the inertia forces caused by the rotation of the outer carrier about each axes of rotation:

$$M_{fx(static)} \succ M_{Cx} \quad , \quad M_{Cx} = I_{Sx}\alpha_{Cx} = I_{Sx}(\alpha_{Sx} - \alpha_{SCx}) \quad (21)$$

$$M_{fy(static)} \succ M_{Cy} \quad , \quad M_{Cy} = I_{Sy}\alpha_{Cy} = I_{Sy}(\alpha_{Sy} - \alpha_{SCy}) \quad (22)$$

$$M_{fz(static)} \succ M_{Cz} \quad , \quad M_{Cz} = I_{Sz}\alpha_{Cz} = I_{Sz}(\alpha_{Sz} - \alpha_{SCz}) \quad (23)$$

where,

α_S …..… Angular acceleration of the rotating structure

α_{SC} …… Angular acceleration of the rotating structure with respect to the carrier

When the actuators rest: $\alpha_{SC} = 0$ and $\alpha_S = \alpha_C$

(4) ***Finally, under the effect of the driving moments from the actuators*****,** to assure the desired rotation of the rotating structure, the summation of the driving moments on each pair of facing rollers should be higher than the summation of both the friction moments opposing this rotation and the inertia moments from the incident carrier rotation

$$M_{driving-el} \succ (M_{fy} + M_{Cy}) \quad , \quad M_{driving-el} = M_{S1} + M_{S2} \tag{24}$$

$$M_{driving-az} \succ (M_{fz} + M_{Cz}) \quad , \quad M_{driving-az} = M_{S3} + M_{S4} \tag{25}$$

SYSTEM'S MATHEMATICAL MODELING

As for the conventional multi-axes ISP, it is convenient to use the mathematical modeling to describe the different kinematics and dynamics phenomena associated to the angular rotation, velocities, accelerations, and torques [9], also, to simulate the designed system to assure the ability of the system to act diligently under the actual working conditions. The arbitrary rotation sequence about the 3-axes can be: *(1)* Absolute rotation about individual axes, *(2)* Simultaneous rotation about two or three axes or *(3)* A combination of absolute rotation about one or more axes followed by a simultaneous rotation about another axes without the stopping of the first rotation, or vise versa. Each of these orders can have positive or negative directions, which results in a huge number of rotations' sequences for only one three dimensional rotation's set.

However, to describe the mathematical model of such system, we have to define one set of rotation's order to deal with. In the upcoming Mathematical Modeling representation, we are going to consider the following rotation sequence, in which; the carrier platform coordinate frame O_P rotates about X_F, Y_F, and Z_F of the fixed inertia reference frame with angular rates of *P*, *Q*, and *R* respectively, and the rotating structure makes a rotation about the -Z-axis of O_P (Azimuth-from Y to X) with an angle (ψ) and angular rate ($\dot{\psi}$), followed by a simultaneous rotation about the -Y-axis (Elevation-from X to Z) with an angle (θ) and angular rate ($\dot{\theta}$) without stopping of the first rotation, as shown in Fig.4.

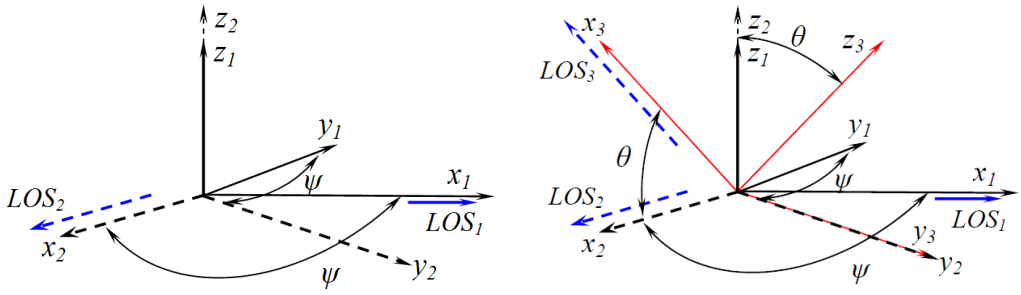

Fig.4. Rotation sequence about Z_1 by angle ψ, then about Y_2 by angle θ

Kinematics Modeling

The carrier platform coordinate's frame is fixed and aligned with that of the enclosure sphere, so, they have the same angular velocity ω_P :

$$\omega_P = \begin{bmatrix} P & Q & R \end{bmatrix}^T \tag{26}$$

Since the rotating structure makes an angular rotation in the Azimuth direction with respect to the carrier platform's coordinate frame with an angular rate (ω_{S-az-p}), it results in an angular velocity of the rotating structure with respect to the fixed inertia reference frame (ω_{S-az}), where, *C* and *S* stand for the Cos and Sin functions respectively,:

$$\omega_{S-az-p} = \begin{bmatrix} 0 & 0 & \dot{\psi} \end{bmatrix}^T \tag{27}$$

$$\omega_{S-az} = E_Z \cdot \omega_P + \omega_{S-az-p} = \begin{bmatrix} PC\psi + QS\psi \\ -PS\psi + QC\psi \\ R + \dot{\psi} \end{bmatrix} \tag{28}$$

The same for the angular rotation of the rotating structure in the Elevation direction with respect to the carrier platform's coordinate frame with an angular rate (ω_{S-el-p}), and with respect to the fixed inertia reference frame (ω_{S-el}). Where, E_y and E_z are the Euler's transformation angles for rotation about the -Y and -Z-axes respectively;

$$\omega_{S-el-p} = \begin{bmatrix} 0 & \dot{\theta} & 0 \end{bmatrix}^T \tag{29}$$

$$\omega_{S-el} = E_Y \cdot \omega_p + \omega_{S-el-p} = \begin{bmatrix} PC\theta - RS\theta \\ Q + \dot{\theta} \\ PS\theta + RC\theta \end{bmatrix} \tag{30}$$

$$E_y(\theta) = \begin{bmatrix} C\theta & 0 & -S\theta \\ 0 & 1 & 0 \\ S\theta & 0 & C\theta \end{bmatrix} \qquad E_z(\psi) = \begin{bmatrix} C\psi & S\psi & 0 \\ -S\psi & C\psi & 0 \\ 0 & 0 & 1 \end{bmatrix} \tag{31}$$

Since the same rotating structure perform the both rotations in the Elevation and Azimuth directions, the total angular velocity of the rotating structure with respect to the fixed inertia reference frame (ω_S) is expressed as following, where (ω_{Sp}) is the relative angular velocity between the rotating structure and the carrier platform;

$$\omega_S = \omega_{S-az} + \omega_{S-el} \quad = (E_z + E_y) \cdot \omega_p + \omega_{Sp} = \begin{bmatrix} P(C\psi + C\theta) + QS\psi - RS\theta \\ -PS\psi + Q(C\psi + 1) + \dot{\theta} \\ PS\theta + R(C\theta + 1) + \dot{\psi} \end{bmatrix} \tag{32}$$

$$\omega_{Sp} = \omega_{S-el-p} + \omega_{S-az-p} = \begin{bmatrix} 0 & \dot{\theta} & \dot{\psi} \end{bmatrix}^T \tag{33}$$

Moreover, the total angular acceleration of the rotating structure with respect to the fixed inertia reference frame (α_S) is obtained by differentiating equation (32):

$$\alpha_S = \dot{\omega}_S = \begin{bmatrix} -P(\dot{\psi}S\psi + \dot{\theta}S\theta) + \dot{P}(C\psi + C\theta) + Q\dot{\psi}C\psi + \dot{Q}S\psi - R\dot{\theta}C\theta - \dot{R}S\theta \\ -P\dot{\psi}C\psi - \dot{P}S\psi - Q\dot{\psi}S\psi + \dot{Q}(1+C\psi) + \ddot{\theta} \\ P\dot{\theta}C\theta + \dot{P}S\theta - R\dot{\theta}S\theta + \dot{R}(1+C\theta) + \ddot{\psi} \end{bmatrix} \quad (34)$$

Kinetics Modeling

From Fig.3, if the structure makes only a rotation about the Y-axis (Elevation), there will not be any rotation's coupling, and the Elevation torque can be expressed as:

$$T_{el} = I_{Sy}\alpha_{Sy} = M_{S1} + M_{S2} - M_{fy} - M_{Cy} \quad (35)$$

If the rotating structure makes a combination of rotations about the three axes, in any sequences, the sum of the Elevation torques considering the coupling effects between the different directions is represented as:

$$T_{el} = (M_{S1} + M_{S2} - M_{fy} - M_{Cy}) + (I_{Sx} - I_{Sz})\omega_{Sx}\omega_{Sz} \quad (36)$$

The same for the Azimuth direction, and From Fig.3, if the rotating structure makes a combination of rotations about the three axes, in any sequences, the sum of the Azimuth torques considering the coupling effects between the different directions is represented as:

$$T_{az} = (M_{S3} + M_{S4} - M_{fz} - M_{Cz}) + (I_{Sx} - I_{Sy})\omega_{Sx}\omega_{Sy} \quad (37)$$

Since this proposed ISP system has one structure performing both the rotations about the Y and Z axes, it eliminates many complexities associated with the mathematical model of the classical two axes Elevation over Azimuth ISP that needs continuous transformation of the angular positions, rates, accelerations and torques from the inner gimbal reference frame to the outer gimbal reference frame and vise versa. This can be clearly shown by comparing the achieved Kinematics and Dynamics equations of this new proposed system with those equations for the same defined sequence of rotations for the classical two axes Elevation over Azimuth ISP discussed in [9].

TWO-AXES ISP BASED ON THE BALL STABILIZATION METHOD

In this section, the Ball Stabilization Method is used, as shown in Figs.5, 6.a and 6.b, for stabilizing and directing the LOS of a Laser Distance Sensor, CMOS camera, motorized zoom lens, red pilot Laser pointer, IR Laser illuminator and electronic clinometers to obtain the range, Yaw, Pitch and Roll angles for each point in the FOV to facilitate Surveillance, Tracking and Ranging of fixed and mobile targets.

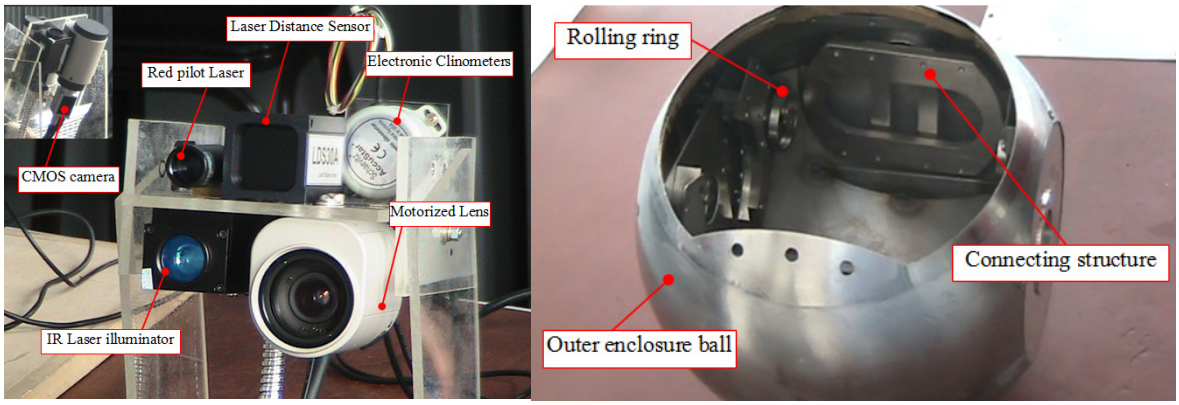

Fig.5. Electro-Optical devices and the outer enclosure sphere

The System Analysis and Validation

The EO sensors were modeled and tested for the optimal masses distribution that achieves minimum inertia forces. The rotating structure, including the EO devices, the driving actuators and the rollers, was designed to be symmetric about each axis of rotation and have an overall mass of about 700 gm. Moreover, the geometric CR is aligned with its CG, which eliminates many complexities of the coupling of rotations about each axis. The enclosure sphere has an outer diameter of 130 mm and inner diameter of 125 mm. While, the four internally machined rolling surfaces have an outer diameter of 130 mm and inner diameter of 120 mm that along with the optical aperture permit the EO devices to have a FOV of ±30º in both the Azimuth and Elevation directions. The principle second moments of inertia of the rotating are:

$$I_x = 0.0008213 \ \ kg/m^2 \ , \quad I_y = 0.0006907 \ \ kg/m^2 \ , \quad I_z = 0.00101 \ \ kg/m^2 \tag{38}$$

Each of the piezoelectric actuators has a dynamic stall force of $T = 4 \ N$ and static hold force of $B = 3.5 \ N$ and the maximum linear velocity of 250 mm/s. The coefficient of static and kinetic friction between the rollers and the rolling surfaces are ($\mu_s = 0.5$) and ($\mu_k = 0.2$) respectively. To assure the optimal performance of the designed stabilization system, the system must pass the conditions mentioned in section 4 as follows:

(1) The 1st condition is already achieved as depicted in equations (1:7) where;

$$F_{1y} = F_{2y} \quad , \quad F_{3z} = F_{4z} \quad , \quad F_{1x} = F_{2x} \quad , \quad F_{3x} = F_{4x} \tag{39}$$

(2) For achieving the 2nd condition, the maximum angular acceleration for the carrier in Elevation and Azimuth rotation directions, α_{Cy} and α_{Cz} respectively, mustn't exceed the following values. Definitely, those values can't be obtained during the regular carrier maneuver and hence guarantees the complete cohesion between the rollers and the rotating structure.

$$\alpha_{Cy} = ((B_1 r_{r1} + B_2 r_{r2}) / I_{Sy}) \approx 121 \ \ rad/s^2 \tag{40}$$

$$\alpha_{Cz} = ((B_3 r_{r3} + B_4 r_{r4}) / I_{Sz}) \approx 83.2 \ \ rad/s^2 \quad (41)$$

Where,

$$r_{r1} = r_{r2} = r_{r3} = r_{r4} = 0.012 \ \ m \quad (42)$$

(3) Also, to achieve the 3rd condition, the maximum angular accelerations for the carrier in the Roll, Elevation and Azimuth rotation directions, α_{Cx} , α_{Cy} and α_{Cz} respectively, mustn't exceed the following values. Again, these maximum angular accelerations for the carrier in all rotation directions can't be obtained during the regular carrier maneuver which guarantees the complete cohesion between the rollers and the inner surface of the enclosure ball.

$$\alpha_{Cx} = (M_{fx(static)} / I_{Sx}) \approx 383.5 \ \ rad/s^2 \quad (43)$$

$$\alpha_{Cy} = (M_{fy(static)} / I_{Sy}) \approx 229.5 \ \ rad/s^2 \quad (44)$$

$$\alpha_{Cz} = (M_{fz(static)} / I_{Sz}) \approx 188 \ \ rad/s^2 \quad (45)$$

(4) From equation (10), the single actuator driving moment ($M_{(S1,S2,S3,S4)} = 0.2057 \ \ N.m$), we can estimate that, the 4th condition requires the maximum angular acceleration for the carrier in the Elevation and Azimuth rotation directions, α_{Cy} and α_{Cz} respectively, shouldn't exceed the following values:

$$\alpha_{Cy} = (((M_{S1} + M_{S2}) - M_{fy}) / I_{Sy}) = ((0.4114 - 0.1585) / 0.0006907) \approx 366 \ \ rad/s^2 \quad (46)$$

$$\alpha_{Cz} = (((M_{S3} + M_{S4}) - M_{fz}) / I_{gz}) = ((0.4114 - 0.19) / 0.00101) \approx 219 \ \ rad/s^2 \quad (47)$$

Again, this maximum angular acceleration for the carrier in both directions can't be obtained during the regular carrier maneuver which guarantees the rotation of the gimbaled structure under the effect of driving forces in one direction without considering the coupling effect of rotation in the other direction.

Finally, to assure the optimal rotation of the gimbaled structure, the exact performance at any rotation angle around the X, Y and Z-axes, under the effect of frictional and external moments from the carrier movement, and under the coupling effect of the different rotations can be estimated easily from equations (36) and (37).

The Total System Performance

For the whole system, the achieved performance has reached a maximum total driving Elevation and Azimuth moments of 411.4 N.mm, a filed of view of ±30º in both directions with a resolution of $1x10^{-5º}$, bandwidth of 1552 Hz, angular rate of $210^{º}$ /s, angular acceleration of $24x10^{3º}$ /s^2 within a compact size of 130 mm in diameter and a total weight of 1.19 kg.

Meanwhile, for the same EO payload, the equivalent classical elevation over Azimuth stabilization system can achieve a filed of view of 360º in Azimuth direction and from -10º to +190º in the Elevation direction with a resolution of $5x10^{-5º}$,

bandwidth of 100 Hz, angular rate of 200º/s, angular acceleration of 100º/s^2 within a 278 x 200 x 256 mm and a total weight of 9.7 kg [14].

Moreover, for the same EO payload, the equivalent Mirror stabilization system can achieve a filed of view of ±0.1º in both directions with a resolution of 0.2x10$^{-5º}$, bandwidth of 3000 Hz, angular rate of 450º/s, angular acceleration of 9x10^{5º}/s^2 within a 75 x 50 x 64 mm and a total weight of 0.25 kg [14].

Compared with the other stabilization methods, the Mass stabilization method has the advantage of the so wide rotation's range. On the other hand, the FSM method has the advantages of high resolution, angular velocity and acceleration, bandwidth, smaller size, and lighter weight, But on the expense of the too small rotation angles. Meanwhile, the Ball stabilization method has an intermediate performance between the above mentioned two methods, which meets the need of many customers for such systems.

The more interesting is the ability to use the Ball Stabilization principle on the outer surface of the ball, as shown in Fig.7.c; in this case, another four driving wheels and piezoelectric edge actuators are strictly connected to the outer surface of the ball in four contacting points resulting in rotating the ball itself in another two orthogonal rotational directions.

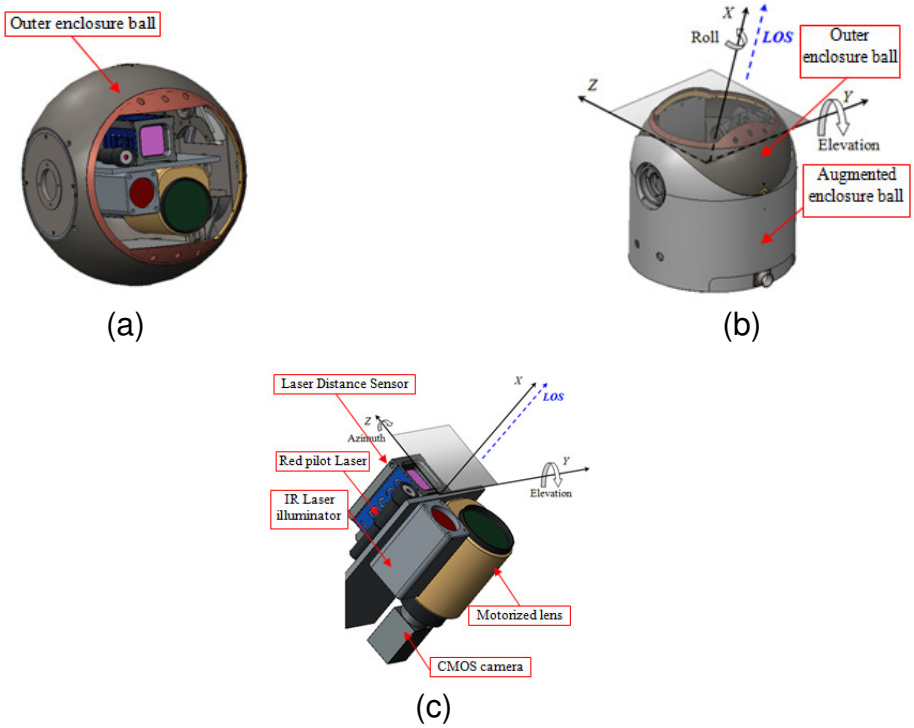

Fig. 6. (a) 3D solid model for the 2-Axis Ball Stabilization ISP, (b) Stabilization about the Y and Z-axes, and (c) Augmented outer Ball Stabilization about the Y and X-axes.

CONCLUSION

The Ball Stabilization method presents a new concept for the EO devices' LOS stabilization. In which, the acquired performance combines the advantages of both

the Mass and Mirror stabilization methods for the wide FOV and the high resolution, angular rates and accelerations. This method eliminates the use of individual gimbals for each direction of rotation through the implementations of the piezoelectric edge actuators where they are strictly connected to the payload and together perform the combined angular rotations inside the spherical enclosure, which permits the miniature design of the overall system and decreases the size and inertia forces and simplifies the system's mathematical model required for further analysis. The designed 2-axis Ball Stabilization ISP has achieved a FOV of ±30º, resolution of $10^{-5º}$, angular rate of $210^{º}$/s, angular acceleration of $24x10^{3º}/s^2$ within a compact size of 130 mm in diameter and a total weight of 1.19 Kg. Moreover, augmented stabilization was also obtained by applying the Ball Stabilization method on both the inner and the outer surfaces of the enclosure ball to achieve four degrees of freedom stabilization. On the other hand, the available piezoelectric edge actuators are still developing only small forces, which limit their applications in stabilization systems to light and moderate payloads.

REFERENCES

[1] Peter J. Kennedy and Rhonda L. Kennedy, "Line of Sight Stabilization Primer", (2009).

[2] J.M. Hilkert, "Inertially Stabilized Platform Technology Concepts And Principles", IEEE Control Systems Magazine, Vol. 28, pp. 26 – 46, (2008).

[3] Peter J. Kennedy and Rhonda L. Kennedy, "Direct Versus Indirect Line of Sight Stabilization", IEEE Transactions on Control Systems Technology, Vol. 11, pp. 3-15, (2003).

[4] Michael. K. Masten, "Inertially Stabilized Platforms for Optical Imaging Systems, Tracking Dynamic Targets With Mobile Sensors", IEEE Control Systems Magazine, Vol. 28, pp. 47 –64, (2008).

[5] A. K. Rue, "Stabilization of Precision Electro-Optical Pointing and Tracking Systems", IEEE Transactions on Aerospace and Electronic Systems, AES-5, pp. 805–819, (1969).

[6] A.K. Rue, "Precision Stabilization Systems", IEEE Transactions on Aerospace and Electronic Systems, AES-10, pp. 34–42, (1974).

[7] Hany F. Mokbel, Lv Qiong Ying, Amr A. Roshdy and Cao Guo Hua, "Design Optimization of the Inner Gimbal for Dual Axis Inertially Stabilized Platform Using Finite Element Modal Analysis", International Journal of Modern Engineering Research, Vol.2, pp. 239-244, (2012).

[8] Zhou Xiangyang, Yu Ruixia, Li Jianping and Li Dapeng, "Structure Optimal Design of Roll Gimbal for an Aerial Three-Axis ISP Based on FEM Modal Analysis", 3rd International Conference on Measuring Technology and Mechatronics Automation, Vol. 3, pp. 373 – 376, (2011).

[9] Hany F. Mokbel, Lv Qiong Ying, Amr A. Roshdy and Cao Guo Hua, "Modeling and Optimization of Electro-Optical Dual Axis Inertially Stabilized Platform", International Conference on Optoelectronics and Microelectronics, pp. 372-377, (2012).

[10] Qingkun Zhou, Pinhas Ben-Tzvi, Dapeng Fan and Andrew A. Goldenberg, "Design of Fast Steering Mirror Systems for Precision Laser Beams Steering", IEEE International Workshop on Robotic and Sensors Environments, (2008).

[11] Daniel J. Kluk, Michael T. Boulet and David L. Trumper, "A High-Bandwidth, High Precision, Two-Axis Steering Mirror with Moving Iron Actuator", Mechatronics, Vol. 22, pp. 257–270, (2012).

[12] Francisc M. Taposa, Derek J. Edingera, Timothy R. Hilbya, Melvin S. Nia, Buck C. Holmesb and David M. Stubbsa, "High Bandwidth Fast Steering Mirror, Optomechanics, Proceedings of SPIE, Vol. 5877, (2005).

[13] Shane Woody and Stuart Smith, "Design and Performance of a Dual Drive System for Tip-Tilt Angular Control of a 300 mm Diameter Mirror", Mechatronics, Vol. 16, pp. 389–397, (2006).

[14] Hany F. Mokbel, Lv Qiong Ying, and Cao Guo Hua, "Optimization of the Mechanical Design of the Dual Axis Inertially Stabilized Platform for the Line of Sight Stabilization", PhD thesis, (2013).